Acta Cryst. (1960). **13**, 434

A Binary Algebra Describing Crystal Structures with Closely Packed Anions.* Part II: A Common System of Reference for Cubic and Hexagonal Structures

BY I. L. MORRIS†

Sylvania, Data Systems Operations, Needham, Mass., U.S.A.

AND A. L. LOEB

Massachusetts Institute of Technology, Department of Electrical Engineering, Cambridge, Mass., U.S.A.

(*Received* 17 *July* 1959)

In the cubic crystals of the rocksalt, sphalerite, antifluorite, and spinel types and in the hexagonal crystals of the nickel arsenide, wurtzite, and olivine types, the cations are either octahedrally or tetrahedrally surrounded. Algorithms are presented here for locating the ions of these seven structures in the following sequence. First, cubically and hexagonally closely packed anion structures are compared, and geometric operators relating the two classes are defined. Second, the location of all possible cation sites is described algebraically, and finally the distribution of cations over these sites is described in terms of the parities of the coordinates of the sites. An interstitial type of crystal model from which the seven classes of crystals have been constructed is discussed.

1. Introduction

In part I of these papers an algebraic description was presented for the location of ions in cubic crystals with closely packed anions (Loeb, 1958), together with calculations of magnetic-dipole interaction energies and the evaluation of neutron diffraction patterns. The purpose of the algebraic description of the three-dimensional patterns formed by various crystal elements is analogous to the aim of analytic geometry, namely to express in a few algorithms the spatial relationships between large numbers of points. Such algorithms, when stored in the memory of an electronic computer, can constitute a crystallographic 'vocabulary' for that computer, to be referred to when certain calculations are to be performed on different types of crystals.

Loeb's (1958) analysis of the olivine structure in analogy with spinel was not altogether successful because spinel has *cubic* symmetry, whereas in olivine the anions form a strongly distorted *hexagonally* closely packed structure rather than a cubic one. The present paper extends the algebra for cubic systems presented in part I to hexagonal ones. This extension is in the nature of a further generalization; the algorithms presented here encompass the following cubic and hexagonal systems; rocksalt, nickel arsenide, sphalerite, wurtzite, anti-fluorite, spinel and olivine.

In all structures under consideration the anions are closely packed, either cubically or hexagonally. Therefore we shall first analyze both closely packed structures, next the interstices between the closely packed ions, and finally the distribution of cations over these interstices.

2. Cubic and hexagonal close-packing; common coordinate system

If the axis of highest symmetry in hexagonally closely packed structures is made to coincide with a 111-axis of the cubic one, then by appropriate scaling and rotation, one third of the planes perpendicular to the common axis can be made coincident; the term 'coincident planes' means that all ion sites in one of the planes coincide with the sites in the other plane. The coincident planes are not uniformly distributed along the common axis, but as adjacent pairs, each pair of coincident planes being separated from the next pair by four non-coincident planes. To describe this less awkwardly, we define the following coordinate system in terms of the Cartesian coordinates used in part I:

$$u = 2x-y-z = 3x-h \quad (1)$$

$$v = -x+2y-z = 3y-h \quad (2)$$

$$w = -x-y+2z = 3z-h \quad (3)$$

$$h = x+y+z \quad (4)$$

where u, v and w are not independent, but are related by (5).

$$u+v+w=0\,. \quad (5)$$

Geometrically, this amounts to the definition of four axes, namely an H-axis along the 111-axis of the cubic structure and three axes U, V and W perpendicular to the H-axis, at angles of 120° with respect to each other. U, V and W are projections of the X-, Y-, and

* This work was supported in part by the U.S. Army (Signal Corps), the U.S. Air Force (Office of Scientific Research, Air Research and Development Command), and the U.S. Navy (Office of Naval Research).

† This work was based partly on an S.M. Thesis submitted to the Department of Electrical Engineering, M.I.T., 1959.

Z-axes, respectively, on an h-plane. The origin is chosen on an anion, and the U-, V- and W-axes go from the origin in the directions of next-nearest anions, as shown in Fig. 1.

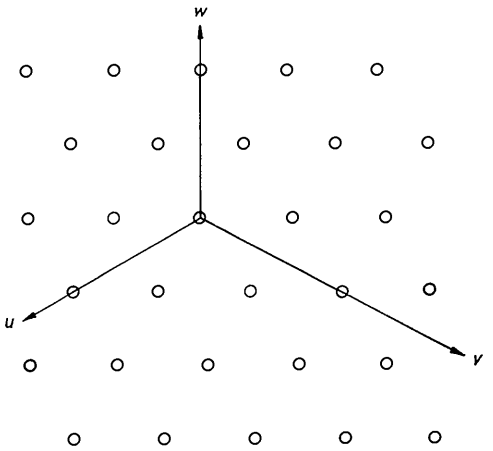

Fig. 1. The U-, V-, and W-axes and the anions in the origin plane.

It was shown that the Cartesian coordinates of the cubically closely packed anions obey the equation

$$x+y+z=2K\,,$$

where K is an integer.

With the aid of equation (4) this is transformed into

$$h=2K\,. \tag{6}$$

From (2) and (3) it follows that, since the Cartesian coordinates of cubically closely packed ions are integers,

$$\left.\begin{aligned} v &= 3L-h_{\text{mod }3} \\ w &= 3M-h_{\text{mod }3} \end{aligned}\right\} \tag{7}$$

where L and M are integers.

[$h_{\text{mod }3} = h-3N$,

where N is an integer so chosen that $|h_{\text{mod }3}| < 3$.]

Since the u-coordinate is related to v and w by (5), it will henceforth not be mentioned explicitly when it is not of special interest.

From (7) it follows that only three types of arrays can occur in any given h-plane, namely those for which (8) holds (called D-planes), those for which (9) holds (called E-planes), and those for which (10) holds (called F-planes).

$$\left.\begin{aligned} v &= 3L \\ w &= 3M \end{aligned}\right\} \tag{8}$$

$$\left.\begin{aligned} v &= 3L+1 \\ w &= 3M+1 \end{aligned}\right\} \tag{9}$$

$$\left.\begin{aligned} v &= 3L-1 \\ w &= 3M-1 \end{aligned}\right\}. \tag{10}$$

These three arrays are shown in Fig. 2(a), projected on a common plane. Accordingly, D-arrays occur in cubically closely packed structures when $h=6N$, E-arrays when $h=6N+2$, and F-arrays when $h=6N-2$, where N is here any integer.

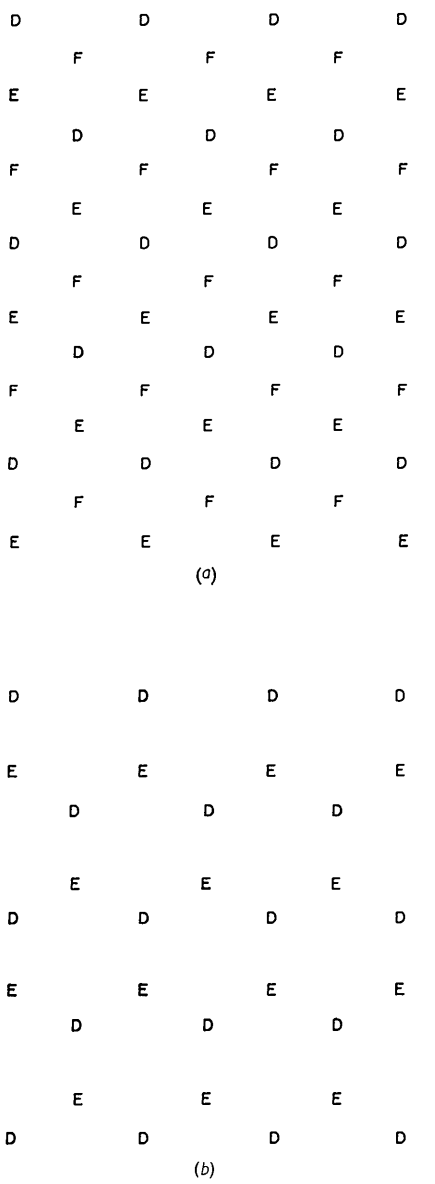

Fig. 2. (a) Projection of cubically closely packed anions on an h-plane. (b) Projection of hexagonally closely packed anions on an h-plane.

For hexagonally closely packed ions we choose the origin in one of the planes coinciding with a plane of the cubic structure, in such a way that the positive h-direction is toward the nearest coincident plane. Then coincident planes occur at $h=0$ and at $h=2$, again at $h=12$ and at $h=14$, etc. Since, in the cubic structures, the planes at $h=0$ and at $h=12$ contain

D-arrays, the same must be true for hexagonal structures. Similarly at $h=2, 14, \ldots, 12N+2$, the hexagonal structures contain E-arrays. The planes at $h=12N\pm4$ and $12N\pm6$ differ for cubically and hexagonally closely packed structures, because, as shown in Fig. 2(b), the hexagonally closely packed structures contain only D- and E-arrays. The stacking of D-, E-, and F-arrays to form cubically and hexagonally closely packed structures is shown in Table 1.

From Fig. 2(a) it follows that when the three arrays are rotated through 60° around an ion belonging to a particular one of the three arrays, that particular array is turned into itself and the other two are turned into each other. An operator $\mathbf{R}(h_0)$ is defined representing rotation of the plane at $h=h_0$ around an ion in that plane, whereas $\mathbf{R}(h_0 \leq h)$ indicates rotation of all planes having $h_0 \leq h$ around an axis through an ion in the plane at $h=h_0$.

Table 1. *Stacking of planes in cubically and hexagonally closely packed structures*

Cubic		Hexagonal
D	$h = 12$	D
F	$h = 10$	E
E	$h = 8$	D
D	$h = 6$	E
F	$h = 4$	D
E	$h = 2$	E
D	$h = 0$	D

The operator $\mathbf{R}(h_0 \leq h)$ is easily applied to demountable crystal models, where it is realized by lifting the portion of the model that is above and includes the plane $h=h_0$, rotating it through 60°, and putting it down again. Tables 2(a) and 2(b) show what happens when the operators

$$\mathbf{R}(2 \leq h),\ \mathbf{R}(4 \leq h),\ \mathbf{R}(6 \leq h),\ \ldots,\ \mathbf{R}(2N \leq h),\ \ldots$$

are successively applied to, respectively, the cubic and hexagonal closely packed structures. In applying these operators, the following rules are observed:

1. $\mathbf{R}(h_0 \leq h)$ does not affect planes with $h<h_0$.
2. $\mathbf{R}(h_0 \leq h)$ leaves unaffected all arrays that are identical with the array at $h=h_0$ and turns the other two types of arrays into each other.

It follows from Tables 2(a) and 2(b) that the sequence

$$\mathbf{R}(2 \leq h),\ \mathbf{R}(4 \leq h),\ \ldots,\ \mathbf{R}(2N \leq h),\ \ldots$$

turns cubic into hexagonal, hexagonal into cubic structures. This relation between hexagonal and cubic crystals is easily demonstrated with demountable models, by using the procedure just given for realizing the operator $\mathbf{R}(h_0 \leq h)$.

3. The interstitial sites

Since any pair of adjacent anion h-planes in the hexagonally closely packed structure can be made to coincide with a pair of h-planes in cubic structures, a description of interstitial sites in terms of adjacent anion planes is applicable to cubic as well as to hexagonal structures. There are two types of interstitial sites, namely those at the centers of octahedra having anions at their corners (octahedral sites), and those at the centers of tetrahedra having anions at their corners (tetrahedral sites). The octahedral sites lie half way between anion planes, with three surrounding anions in one anion plane, and three anions in the other anion plane. The tetrahedral sites lie half way between octahedral-site planes and anion planes, with three surrounding anions in the nearest anion plane that

Table 2(a). *Conversion of the cubic into the hexagonal closely packed structure*

Result of applying the operator $\mathbf{R}(h_0 \leq h)$ to the previous column

h	Cubic	$\mathbf{R}(2 \leq h)$	$\mathbf{R}(4 \leq h)$	$\mathbf{R}(6 \leq h)$	$\mathbf{R}(8 \leq h)$	$\mathbf{R}(10 \leq h)$	$\mathbf{R}(12 \leq h)$
0	D	D	D	D	D	D	D
2	E	E	E	E	E	E	E
4	F	D	D	D	D	D	D
6	D	F	E	E	E	E	E
8	E	E	F	D	D	D	D
10	F	D	D	F	E	E	E
12	D	F	E	E	F	D	D
14	E	E	F	D	D	F	E

Table 2(b). *Conversion of the hexagonal into the cubic closely packed structure*

Result of operating on the previous column with the operator $\mathbf{R}(h_0 \leq h)$

h	Hexagonal	$\mathbf{R}(2 \leq h)$	$\mathbf{R}(4 \leq h)$	$\mathbf{R}(6 \leq h)$	$\mathbf{R}(8 \leq h)$	$\mathbf{R}(10 \leq h)$	$\mathbf{R}(12 \leq h)$
0	D	D	D	D	D	D	D
2	E	E	E	E	E	E	E
4	D	F	F	F	F	F	F
6	E	E	D	D	D	D	D
8	D	F	F	E	E	E	E
10	E	E	D	D	F	F	F
12	D	F	F	E	E	D	D
14	E	E	D	D	F	F	E

forms the base of the tetrahedron, and the fourth anion that forms the apex of the tetrahedron in the next-nearest anion plane. The distance from a tetrahedral site to its nearest anion plane is one third of the distance to its next-nearest anion plane; this agrees with the geometry of the equilateral tetrahedron. Table 3 summarizes the occupation of various h-planes by anions and interstitial sites.

Table 3. *Stacking of anions, A-sites, and B-sites in cubic and hexagonal structures*

Cubic		Hexagonal
D	$h = 12$	D
F	$h = \frac{23}{2}$	E
E	$h = 11$	F
D	$h = \frac{21}{2}$	D
F	$h = 10$	E
E	$h = \frac{19}{2}$	D
D	$h = 9$	F
F	$h = \frac{17}{2}$	E
E	$h = 8$	D
D	$h = \frac{15}{2}$	E
F	$h = 7$	F
E	$h = \frac{13}{2}$	D
D	$h = 6$	E
F	$h = \frac{11}{2}$	D
E	$h = 5$	F
D	$h = \frac{9}{2}$	E
F	$h = 4$	D
E	$h = \frac{7}{2}$	E
D	$h = 3$	F
F	$h = \frac{5}{2}$	D
E	$h = 2$	E
D	$h = \frac{3}{2}$	D
F	$h = 1$	F
E	$h = \frac{1}{2}$	E
D	$h = 0$	D

——— anion planes
– – – – – – – tetrahedral-site planes
– – – – – octahedral-site planes

It follows that all octahedral sites must satisfy the equation

$$h = 2K + 1 \tag{11}$$

and tetrahedral sites must satisfy either

$$h = 2K + \tfrac{1}{2} \tag{12a}$$

or

$$h = 2K - \tfrac{1}{2}\,. \tag{12b}$$

If the interstitial sites of two adjacent anion planes are projected on these anion planes, some interesting relationships are revealed. The octahedral sites project on the centers of the triangles formed by the anions of both nearest anion planes, so that the array formed by the octahedral sites differs from that formed by the anions in the nearest planes (see Table 3). The tetrahedral sites project on those anions that form the apices of their surrounding tetrahedra. The arrays formed by the tetrahedral sites are therefore identical with those in the next-nearest anion planes, and hence differ from arrays in both adjacent planes, one plane of which contains anions and one of which contains octahedral sites (see Table 3).

4. Summarizing algorithms for the location of closely packed ions and interstitial sites

Table 3 summarizes graphically the location of the ions and interstices in cubic and hexagonal closely packed structures. This information can be expressed more generally in terms of the following algorithms, which can be easily programmed for a digital computer.

The equations for the location of both ions and interstices are:

$$\left.\begin{aligned} v &= 3L + [f(h)]_{\text{mod }3} \\ w &= 3M + [f(h)]_{\text{mod }3} \end{aligned}\right\} \tag{13}$$

where

$$f(h) = 2h \text{ for cubic structures} \tag{14}$$

and

$$f(h) = 4 - 2|h_{\text{mod }4} - 2| \text{ for hexagonal structures}\,. \tag{15}$$

The planes $h = 2K$ are occupied by anions.

The planes $h = 2K + 1$ are occupied by octahedral interstices.

The planes $h = 2K \pm \frac{1}{2}$ are occupied by tetrahedral interstices.

The h-planes having $[f(h)]_{\text{mod }3} = 0$ contain D-arrays.
The h-planes having $[f(h)]_{\text{mod }3} = 1$ contain E-arrays.
The h-planes having $[f(h)]_{\text{mod }3} = 2$ contain F-arrays.

As an example, let us use these algorithms to determine the configuration in the plane $h = 15/2$ for both the cubic and hexagonal structures and compare the results with Table 3.

For cubic structures $f(15/2) = 15$, therefore

$$f(15/2)_{\text{mod }3} = 0;$$

therefore the plane $h = 15/2$ contains a D-array. Since $15/2 = 2K - \frac{1}{2}$, the plane $h = 15/2$ contains tetrahedral sites.

For hexagonal structures $f(15/2) = 4 - 2|\frac{7}{2} - 2| = 4 - 3 = 1$; therefore the plane $h = 15/2$ contains an E-array of tetrahedral sites.

Both of these results agree with Table 3. Note that, at first sight, it might appear that (7) and (14) contradict each other. However, $(2h)_{\text{mod }3} = -h_{\text{mod }3}$; although (7) describes the anion locations in cubic crystals, it does not describe the locations of the interstitial sites. Equation (14) is valid for *all* ions and *all* interstitial sites.

5. Rocksalt, sphalerite, nickel arsenide, wurtzite and fluorite

The classes of crystal structures under consideration here all have closely packed hexagonal or cubic anion

structures and differ in the distribution of cations over the interstitial sites. A complete description of the crystal structures consists of the algorithms of section 4 together with a description of the distribution of ions over the interstitial sites. The latter is given in the form of a distribution pattern, in which all possible sites are described by 0 (empty) or 1 (filled).

Table 4. *Distribution pattern for rocksalt and nickel arsenide*

$h=2K-\frac{1}{2}$	0
$h=2K+1$	1
$h=2K+\frac{1}{2}$	0

The distribution pattern for rocksalt (NaCl) and nickel arsenide (NiAs) are shown in Table 4, which indicates that in both of these structures all tetrahedral sites are empty and all octahedral sites are filled.

Both sphalerite and wurtzite have half of their tetrahedral sites filled, and all other sites empty; there are two possible distribution patterns, as shown in Table 5.

Table 5. *Distribution patterns for sphalerite and wurtzite*

$h=2K-\frac{1}{2}$	1		$h=2K-\frac{1}{2}$	0
$h=2K+1$	0	or	$h=2K$	0
$h=2K+\frac{1}{2}$	0		$h=2K+\frac{1}{2}$	1

Table 6. *Distribution pattern for anti-fluorite*

$h=2K-\frac{1}{2}$	1
$h=2K+1$	0
$h=2K+\frac{1}{2}$	1

The antifluorite structure consists of closely packed anions with, for instance, potassium ions in all tetrahedral sites. Its distribution pattern is shown in Table 6.

It follows that four binary digits are sufficient to store all information regarding these five crystal structures in a computer memory; namely, three for the distribution pattern, and one to distinguish hexagonal from cubic patterns in order to refer the computer to the appropriate computation for $f(h)$. In addition to these four bits the algorithms of section 4 must be stored as standard subprograms in the permanent vocabulary of the computer.

6. Further subdivision of interstitial sites; exchange coupling

In part I the octahedral sites were subdivided into subarrays for two reasons. In antiferromagnets of the rocksalt these sites are occupied by four sets of dipoles; exchange coupling between any pair of dipoles occurs only if the two dipoles belong to the same set. Therefore it is important to indicate not only whether or not octahedral sites are filled, but also to which set of the four sets of dipoles the cation occupying it belongs. Secondly, in spinel and olivine only a fraction of the sites in any given h-plane is occupied; it is therefore necessary to indicate which sites within any h-plane are filled, and which are empty. Both for the description of the four dipole systems and for that of spinel the octahedral sites were subdivided according to the parities of their y- and z-coordinates. The four subarrays are called 'a', 'b', 'c' and 'd', and are defined by Table 7, where '0' indicates 'even' and '1' indicates 'odd'.

Table 7. *Subdivision of octahedral sites according to their y- and z-parity*

$y_{\text{mod }2}$, $z_{\text{mod }2}\rightarrow$			
00	01	11	10
a	b	c	d

Table 7 can be rewritten in terms of v and w with the aid of (2) and (3). Since $3y$ and $3z$ have the same respective parities as do y and z, and since for octahedral sites h is odd, the parities of v and w are opposite to those of y and z, respectively. The result is shown as Table 8; the use of this table will be extended to subdivide the anions and the tetrahedral sites as well.

Table 8. *Subdivision of sites according to their v- and w-parity*

$v_{\text{mod }2}$, $w_{\text{mod }2}\rightarrow$			
11	10	00	01
a	b	c	d

In the cubic rocksalt-like antiferromagnets, exchange coupling occurred only between dipoles having the same set of v- and w-parities, with all dipoles at sites with even K antiparallel to those at sites with odd K. As an example of the application of the algorithms presented in this paper, we shall compute the exchange angle for the hexagonal nickel arsenide structure. Exchange coupling between dipoles on cations occurs through an anion, and is strongest when the cation–anion–cation angle is closest to 180°. The coupling strength not only decreases with decreasing angle, but also with increasing cation–anion distances. Let us consider exchange coupling through the anion at the origin; coupling through any other anion follows the same pattern. At the origin $h=0$, $v=0$, $w=0$; from Table 8 it follows that the anion at the origin belongs to the 'c' subarray. For hexagonal structures the octahedral sites all occupy F-arrays, so that they have $v=3L-1$, $w=3M-1$. The cations nearest the origin lie in the planes $h=1$ and $h=-1$; their v and w coordinates are therefore combinations of 2 and -1. The six cations nearest the origin are listed in Table 9; it is seen that the cations of the 'c' array are not represented among the nearest six. It is generally true that anion–cation distances are smaller when the two ions have different sets of v and w parities, than when

both v and w parities are the same. The u, x, y and z coordinates listed in Table 9 are found from h, v and w with the aid of equations (1)–(5).

Table 9.* *Coordinates of cations nearest origin for* NiAs *structure*

Cation	h	v	w	u	x	y	z
a	1	−1	−1	2	1	0	0
b	1	−1	2	−1	0	0	1
d	1	2	−1	−1	0	1	0
a'	−1	−1	−1	2	$\frac{1}{3}$	$-\frac{2}{3}$	$-\frac{2}{3}$
b'	−1	−1	2	−1	$-\frac{2}{3}$	$-\frac{2}{3}$	$\frac{1}{3}$
d'	−1	2	−1	−1	$-\frac{2}{3}$	$\frac{1}{3}$	$-\frac{2}{3}$
c	1	2	2	−4	−1	1	1
c'	−1	2	2	−4	$-\frac{5}{3}$	$\frac{1}{3}$	$\frac{1}{3}$

If we call the vectors from the origin to the nearest a '**a**', that to the nearest b '**b**', etc., we can find the cosine of the angle subtended by any pair of cations at the origin by taking the scalar product of the vectors going to each of the cations:

$$\cos(\mathbf{a}, \mathbf{a}') = \frac{\mathbf{a}.\mathbf{a}}{|\mathbf{a}||\mathbf{a}'|} = \frac{(\frac{1}{3})+0+0}{1.[(\frac{1}{3})^2+(-\frac{2}{3})^2+(-\frac{2}{3})^2]^{\frac{1}{2}}} = \frac{1}{3}.$$

Similarly it is shown that $\cos(\mathbf{b}, \mathbf{b}') = \cos(\mathbf{d}, \mathbf{d}') = \frac{1}{3}$.

$$\cos(\mathbf{a}, \mathbf{b}') = -\tfrac{2}{3} = \cos(\mathbf{a}, \mathbf{d}') = \cos(\mathbf{b}, \mathbf{d}').$$
$$\cos(\mathbf{a}, \mathbf{b}) = 0 = \cos(\mathbf{a}', \mathbf{b}') = \cos(\mathbf{a}, \mathbf{d}).$$

The largest angles are the ones whose cosines are $-\frac{2}{3}$, that is, angles of 131° 46′; exchange coupling therefore is not as strong in the NiAs structure as it is in the rocksalt structure, where the angle is 180°. The angle 131° 46′ occurs in nickel arsenide whenever the two cations and the anion involved in the coupling each have a different set of v- and w-parities. Each cation has six nearest anions belonging to subarrays different from its own; each of these anions has two nearest cations belonging to subarrays different from both the anion and the first cation. Therefore each cation is coupled through an angle of 131° 46′ to twelve other cations that all have sets of v- and w-parities different from its own. This contrasts with the coupling in rocksalt, in which each cation is coupled through an angle of 180° to six other cations with the same set of v- and w-parities.

7. Spinel

In part I it was shown that, in spinel, one half of all octahedral and one eighth of all tetrahedral interstices between cubically closely packed anions are occupied. The results of part I are expressed in the distribution pattern of Table 10, where the distribution of ions within the various h-planes is expressed as a function of v and w. It was stated in part I that there are many equivalent distributions of ions, differing from each other only in rotation. This equivalence is a function of the symmetry properties of the cubic system. The distribution pattern should be sufficiently general to include all equivalent distributions; for this reason, the rows in Table 10 are labeled in terms of the value of $(h-2K_0)$, where K_0 is an integer. If K_0 is even, then the rows $h-2K_0=1, 5, 9$, etc. correspond to the planes containing the sites that were unprimed in part I, while those having $h-2K_0=3, 7, 11$, etc. correspond to those sites that were primed in part I. If K_0 is chosen odd, then the primed and unprimed sites are interchanged. The columns in Table 10 are not separately labelled, for any assignment of the binary numbers zero through three will do. If, for instance, the four columns are labeled successively 11, 10, 00, 01, then they represent respectively a, b, c, and d sites (see Table 10). On the other hand the assignment (00, 11, 10, 01) would correspond to the sequence c, a, b, d. Since there are twenty-four ways of labeling the column headings, and K_0 may be chosen either even or odd, there would be altogether forty-eight different but equivalent ways of labeling the entries in Table 10.

Table 10. *Distribution pattern in spinel*

$(h-2K_0)_{\text{mod }4}\rightarrow$ \ $(v_{\text{mod }2}, w_{\text{mod }2})\rightarrow$					
$\frac{7}{2}$	0	0	0	1	▽
3	0	0	0	1	
$\frac{5}{2}$	0	0	0	1	△
2	0	0	0	0	▽
1	1	1	1	0	
$\frac{1}{2}$	0	0	0	0	△

It is of interest to apply to Table 10 the observations, made in section 6, that ions and sites having the same set of v- and w-parities are never nearest neighbors. We conclude from the distribution pattern of Table 10 that:

(*a*) The h-planes containing octahedral sites are alternately more and less densely populated.

(*b*) Only h-planes adjoining the less densely populated octahedral-site planes are occupied by tetrahedrally coordinated cations.

(*c*) The tetrahedral sites are occupied such that the average separation of ions is a maximum, hence the electrostatic repulsion a minimum.

In Table 10 the triangles in the tetrahedral-site planes indicate whether the tetrahedral sites have their apex pointing in the positive (△) or negative (▽)h-direction.

8. Olivine

In olivine, as in spinel, one half of all octahedral and one eighth of all tetrahedral sites are occupied. Olivine differs from spinel in two respects, however. In the first place, the anions are more nearly hexagonally than cubically closely packed, and in the second place, the distribution pattern is different. In olivine the cations are more uniformly distributed

* Primes indicate odd values of K, as defined in part I.

along the H-axis than in spinel, with each octahedral-site plane half-occupied, and each tetrahedral-site plane one-eighth occupied. This means that the four arrays in each h-plane must each be divided into two halves, with a resulting loss of symmetry. In making the further subdivision, one of the three axes perpendicular to the H-axis is singled out in preference to the other two, and as a result the cation distribution in olivine has orthorhombic symmetry. Although the anion structure has hexagonal symmetry, the symmetry of olivine is orthorhombic.

In drawing a distribution pattern for olivine we find that, as a result of the lower symmetry, the four subarrays a, b, c, and d are no longer equivalent to each other. Suppose that the three axes of the orthorhombic structure are oriented in such a way that two axes coincide with the H- and W-axes, respectively, of our coordinate system, with the third axis normal to both of these, lying in an h-plane at angles of 30° and 150° with respect to the V- and U-axes. Then the W-axis is singled out as unique, and the four subarrays are further subdivided into halves according to their w-coordinate. In each h-plane the ion sites are separated from each other by integer multiples of three units of w. In D-planes the b- and c-arrays have sites located at $w=6N$, where N is an integer, because for these arrays, w is even (see Table 8). Similarly, the a- and d-arrays have sites located at $w=6N+3$ in D-planes, since they must have odd values of w (see Table 8). Similarly, in E-planes the b and c arrays have sites with $w=6N+4$, and a and d sites with $w=6N+1$, while for F-arrays, the b and c arrays occupy the lines $w=6N+2$, and the a and d arrays the lines $w=6N+5$. Thus the periodicity of the sites in any given h-plane is six units of w. In olivine the distribution of ions over these sites is such that the structure has a periodicity in any h-plane of twelve units in w. This means that, for instance, in a D-plane the line $w=0$ has a different distribution of ions over its b- and c-sites than does the line $w=6$, but the same distribution as the line $w=12$, or, indeed, any line $w=12N$. Thus we assign subscripts '1' and '2' according to the following definitions:

In D-planes the sites of arrays a_1 and d_1 have $w=12N+3$.
In D-planes the sites of arrays a_2 and d_2 have $w=12N+9$.
In D-planes the sites of arrays b_1 and c_1 have $w=12N+6$.
In D-planes the sites of arrays b_2 and c_2 have $w=12N+12$.

In E-planes the sites of arrays a_1 and d_1 have $w=12N+1$.
In E-planes the sites of arrays a_2 and d_2 have $w=12N+7$.
In E-planes the sites of arrays b_1 and c_1 have $w=12N+4$.
In E-planes the sites of arrays b_2 and c_2 have $w=12N+10$.

In F-planes the sites of arrays a_1 and d_1 have $w=12N+5$.
In F-planes the sites of arrays a_2 and d_2 have $w=12N+11$.
In F-planes the sites of arrays b_1 and c_1 have $w=12N+2$.
In F-planes the sites of arrays b_2 and c_2 have $w=12N+8$.

In the summary given in Table 11, it is observed that the subscript '1' is attached to all sites having $12N<w\leq 12N+6$, the subscript '2' to all sites having $12N+6<w\leq 12N+12$. The distribution pattern over these eight arrays is shown in Table 12; just as in spinel, the coordinate along the h-axis is expressed as $(h-2K_0)$. The column headings are no longer immaterial because the four arrays a, b, c and d are no longer completely symmetrical with respect to each other. They are therefore labeled so as to distinguish their v- and w-parities; the symbol '$\sim$' indicates

Table 11. *Definition of subarrays of ionic and interstitial sites in olivine*

	Arrays		
w	Even v	Odd v	Type of plane
$12N+1$	d_1	a_1	E
$12N+2$	c_1	b_1	F
$12N+3$	d_1	a_1	D
$12N+4$	c_1	b_1	E
$12N+5$	d_1	a_1	F
$12N+6$	c_1	b_1	D
$12N+7$	d_2	a_2	E
$12N+8$	c_2	b_2	F
$12N+9$	d_2	a_2	D
$12N+10$	c_2	b_2	E
$12N+11$	d_2	a_2	F
$12N+12$	c_2	b_2	D

Table 12. *Distribution pattern for olivine*

	v		$\tilde{w}$		$\tilde{v}$		w		
	w		$\tilde{w}$		w		$\tilde{w}$		
	1	2	1	2	1	2	1	2	
$(h-2K_0)_{\mathrm{mod}\,4}\rightarrow$									
$\frac{7}{2}$	0	0	0	0	0	0	0	1	▽
3	0	0	1	0	1	0	1	1	
$\frac{5}{2}$	0	0	0	0	0	0	0	1	△
				*					
$\frac{3}{2}$	1	0	0	0	0	0	0	0	▽
1	1	1	0	1	0	1	0	0	
$\frac{1}{2}$	1	0	0	0	0	0	0	0	△

binary complementation, so that if v equals zero, $\tilde{v}$ equals unity, and if w equals unity, $\tilde{w}$ equals zero. If we choose, for instance, $v=1$ and $w=0$, then the columns in Table 12 represent the arrays b_1, b_2, a_1, a_2, d_1, d_2, c_1, c_2. It is interesting to note that the point marked * in Table 12 is a point of inversion in the distribution pattern for olivine.

Table 12 can be stated in words by passing along the H-axis starting at the origin:

$(h-2K_0)_{\text{mod }4}=0$:
Completely filled anion plane.

$(h-2K_0)_{\text{mod }4}=\frac{1}{2}$:
One subarray occupied.

$(h-2K_0)_{\text{mod }4}=1$:
Four subarrays occupied, two having the same v- and w-parities as the one at $(h-2K_0)_{\text{mod }4}=\frac{1}{2}$, while the other two both have opposite w-parities and opposite subscripts from the one having $(h-2K_0)_{\text{mod }4}=\frac{1}{2}$.

$(h-2K_0)_{\text{mod }4}=\frac{3}{2}$:
The same subarray occupied, as at $(h-2K_0)_{\text{mod }4}=\frac{1}{2}$.

$(h-2K_0)_{\text{mod }4}=2$:
Completely filled anion plane.

$(h-2K_0)_{\text{mod }4}=\frac{5}{2}$:
One subarray occupied, having the same w-parity but opposite v-parity and subscript as the one at $(h-2K_0)_{\text{mod }4}=\frac{1}{2}$.

$(h-2K_0)_{\text{mod }4}=3$:
Those four subarrays that were unoccupied at $(h-2K_0)_{\text{mod }4}=1$, occupied.

$(h-2K_0)_{\text{mod }4}=\frac{7}{2}$:
One subarray occupied, having the same w-parity, but opposite v-parity and subscript, as the one occupied in the plane $(h-2K_0)_{\text{mod }4}=\frac{1}{2}$.

9. Summary and concluding remarks

A mathematical method has been devised for describing the location of all ions in crystal structures having either hexagonally or cubically closely packed anions. This method is quite suitable in the development of a vocabulary of crystal structures for digital computers. It is interesting to compare the number of binary digits necessary for storing the spatial concepts with the number of digits necessary for storing the name of the crystal. The number of digits necessary for storing a letter in a computer memory can be taken as $\log_2 26$, which is approximately 4.7. Thus the word 'spinel,' which contains six letters, requires approximately twenty-eight binary digits, while the word 'olivine' requires thirty-three binary digits. From Tables 10 and 12 it follows that the concepts 'spinel' and 'olivine' require twenty-five and forty-nine binary digits, respectively, that is, one more than the number of digits shown in those tables in order to tell the computer whether the structures are hexagonal or cubic. For simpler structures, such as rocksalt and sphalerite, the conceptual description requires far less memory space than does the literal one. More important, of course, is the fact that the conceptual description is suitable for computation because it has physical significance, while the literal one is not.

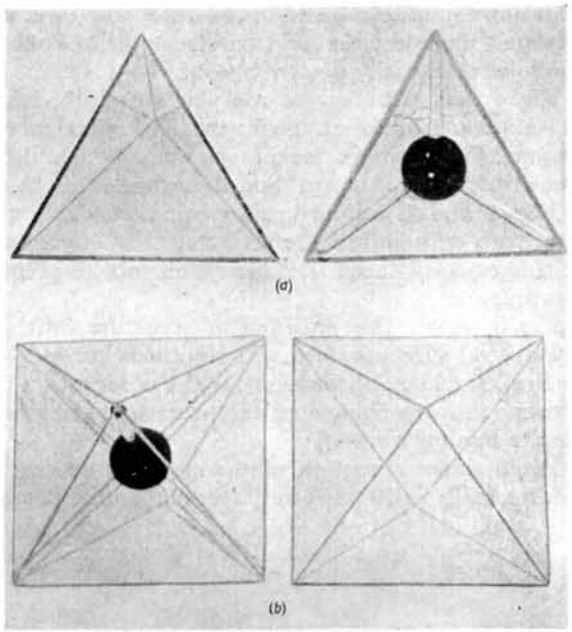

Fig. 3. Modules for interstitial models.

The analysis has led, furthermore, to the invention of interstitial crystal models. Of the four modules shown in Fig. 3, the seven structures discussed in this paper have been constructed with the aid of the distribution patterns. Each of the modules shown represents an interstice between closely packed anions; the anions are not shown explicitly, but are at the corners of the polyhedra. Occupied cation sites are shown by a sphere at the center of the polyhedron, empty sites by an empty polyhedron. Close-packing is easily demonstrated by showing that the tetrahedra and octahedra together can occupy all of space; the difference between cubic and hexagonal close-packing

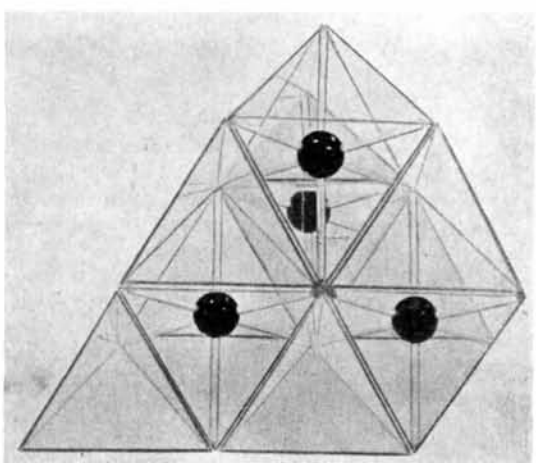

Fig. 4. Interstitial model of rocksalt.

is demonstrated by placing tetrahedra on top of octahedra and octahedra on top of tetrahedra in the cubic case, and octahedra on top of octahedra, and tetrahedra on top of tetrahedra in the hexagonal case, with adjacent modules sharing a triangular face. Pauling's rules are thus easily demonstrated.

Fig. 4 demonstrates the rocksalt structure, with a 111-axis vertical. All octahedra are filled, all tetrahedra empty. Fig. 5 shows nickel arsenide, which differs from rocksalt by the rotation described in section 2.

Figs. 6 and 7, similarly, show sphalerite and wurtzite, with only half of the tetrahedral sites occupied; in this case, all those that have their apices pointing upward.

Fig. 8 shows the antifluorite structure, with all tetrahedral sites occupied. [The authors are indebted to Prof. David P. Shoemaker for the observation that rotation into the hexagonal analogue would flagrantly violate Pauling's rules.]

Fig. 9 shows a portion of the spinel structure; according to Table 10 the lower layer of modules contains three times as many filled as empty octahedra, while the upper layer contains three times as many empty as filled octahedra. Table 10 indicates also that in the

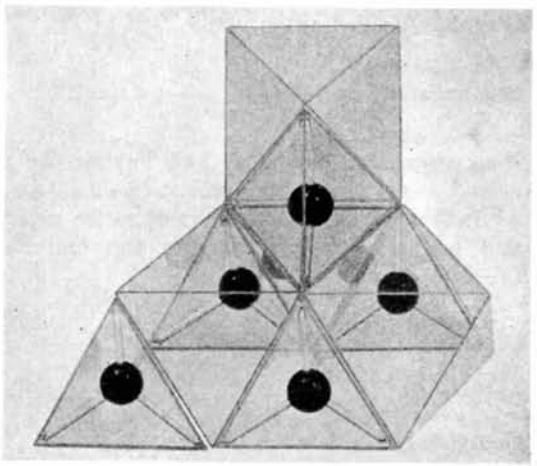

Fig. 7. Interstitial model of wurtzite.

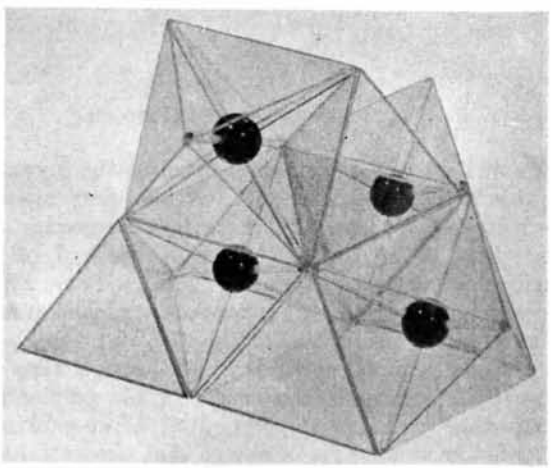

Fig. 5. Interstitial model of nickel arsenide.

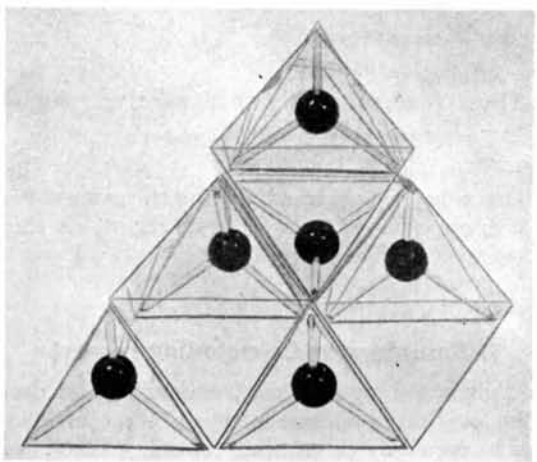

Fig. 8. Interstitial model of antifluorite.

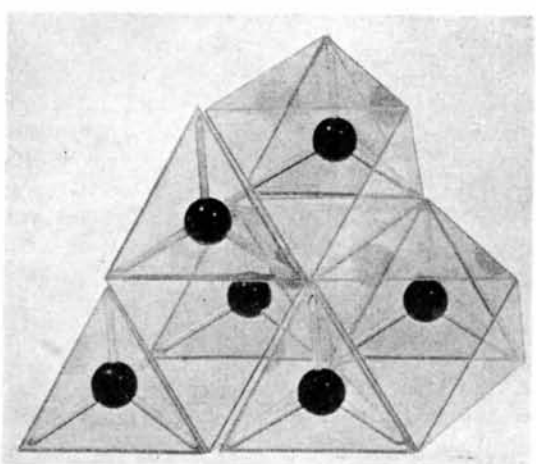

Fig. 6. Interstitial model of sphalerite.

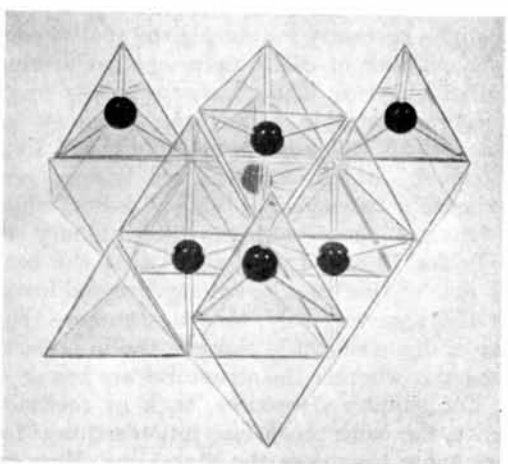

Fig. 9. Interstitial model of spinel.

portion shown filled tetrahedra sit on empty octahedra, and empty tetrahedra sit on filled octahedra, as can be confirmed by comparing the occupation of the tetrahedral site plane $(h-2K_0)_{\text{mod }4}=5/2$ with that of the octahedral site plane $(h-2K_0)_{\text{mod }4}=1$.

The olivine structure, which is similarly constructed, is shown in Fig. 10.

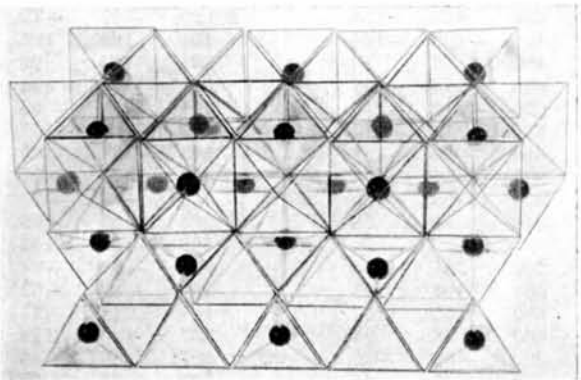

Fig. 10. Interstitial model of olivine.

In these models the tetrahedrally surrounded ions are represented by red, the octahedrally surrounded ions by blue spheres.

The interstitial models have the advantage of flexibility, since they are self-supporting and do not need interlocking mechanisms. The rods supporting the spheres actually represent the anion–cation bonds, the corners at which all edges converge, the anions, so that the structures owe their support to physically meaningful elements. Therefore these models can be used to show many crystal structures and, especially, the relationships between these structures. They are invaluable for deriving and checking the distribution patterns.

The authors are indebted to Mr Ralph Casale for his assistance and guidance in constructing the four types of modules, and to Mr Stuart Bemis for making the photographs shown in Figs. 3 through 10.

Reference

LOEB, A. L. (1958). *Acta Cryst.* **11**, 469.

Acta Cryst. (1960). **13**, 443

The Crystal Structure of $KReO_4$

BY J. C. MORROW

Department of Chemistry, University of North Carolina, Chapel Hill, North Carolina, U.S.A.

(*Received* 6 *July* 1959 *and in revised form* 12 *October* 1959)

Single crystals of $KReO_4$ have been examined by means of X-ray diffraction in order to determine the location of oxygen atoms in the unit cell. The unit-cell dimensions have been redetermined and found to be:

$$a=5{\cdot}680\pm0{\cdot}002,\ c=12{\cdot}703\pm0{\cdot}006\ \text{Å}\ .$$

The space group is $I4_1/a$ with 4 K and 4 Re in special positions and 16 O in general positions corresponding to $x=0{\cdot}131$, $y=0{\cdot}041$, $z=0{\cdot}210$. Oxygen atoms form nearly regular tetrahedra around Re. The Re–O separation suggests considerable double bond character for this bond.

Introduction

Shortly after the isolation of rhenium, Broch (1929) examined $KReO_4$ powder with Cu $K\alpha$ radiation and proposed that the salt is isomorphous with scheelite, $CaWO_4$. The present work was begun to determine the locations of the oxygen atoms in $KReO_4$, for which purpose diffraction by single crystals is required.

Experimental procedure

Pure $KReO_4$, obtained from the Department of Chemistry of the University of Tennessee, was used to prepare a water solution from which tetragonal octahedra were deposited on slow evaporation of the solvent. The specimen used for b-axis rotation had a length of 115·5 microns; its maximum cross-section was a square with side 63·0 microns. For c-axis rotation the crystal selected had corresponding dimensions of 76·1 microns and 34·4 microns. For both crystals, diffraction of Zr-filtered Mo $K\alpha$ radiation was recorded by the Weissenberg and precession methods.

Kodak No-screen and Blue Brand film, six sheets in depth, were employed for the recording of equatorial Weissenberg photographs. Intensities were estimated visually by comparison with timed exposure scales produced by the diffracting crystal. Since the small Bragg angle of (101) prevented its being recorded by